

See discussions, stats, and author profiles for this publication at: <https://www.researchgate.net/publication/6524446>

Influence of a Reduced Mobility Layer on the Structural Relaxation Dynamics of Aluminum Capped Ultrathin Films of Poly(ethylene terephthalate)

ARTICLE in LANGMUIR · MARCH 2007

Impact Factor: 4.46 · DOI: 10.1021/la062229j · Source: PubMed

CITATIONS

45

READS

29

6 AUTHORS, INCLUDING:



Simone Napolitano

Université Libre de Bruxelles

45 PUBLICATIONS 1,001 CITATIONS

SEE PROFILE



Pasqualantonio Pingue

Scuola Normale Superiore di Pisa

49 PUBLICATIONS 505 CITATIONS

SEE PROFILE



Mario D'Acunto

Italian National Research Council

59 PUBLICATIONS 459 CITATIONS

SEE PROFILE



P. A. Rolla

Università di Pisa

114 PUBLICATIONS 2,118 CITATIONS

SEE PROFILE

Influence of a Reduced Mobility Layer on the Structural Relaxation Dynamics of Aluminum Capped Ultrathin Films of Poly(ethylene terephthalate)

Simone Napolitano,^{†,||} Daniele Prevosto,[†] Mauro Lucchesi,[†] Pasqualantonio Pingue,[‡] Mario D'Acunto,[§] and Pierangelo Rolla^{*,†}

polyLab e Dipartimento di Fisica, Università di Pisa, Largo B. Pontecorvo 3, Pisa, Italy, NEST CNR-INFM and Scuola Normale Superiore, I-56100, Pisa, Italy, Dipartimento Ingegneria Chimica e Scienze dei Materiali, Università di Pisa, via Diotisalvi 2, Pisa, Italy, and Laboratory for Acoustics and Thermal Physics, Department of Physics and Astronomy, Katholieke Universiteit Leuven, Celestijnenlaan 200D B-3001 Heverlee, Belgium

Received July 28, 2006. In Final Form: September 28, 2006

The structural dynamics of ultrathin polymer films of poly(ethylene terephthalate) capped between aluminum electrodes have been investigated by dielectric relaxation spectroscopy. A deviation from bulk behavior, appearing as an increase of the relaxation time at a fixed temperature, is observed for films of thickness below 35 nm. The slowing down acts as a constant shift factor independent from the temperature, and the fragility is constant. The interfacial energy between aluminum and poly(ethylene terephthalate) is calculated to be 3 mJ/m², confirming a strong interaction between polymer and substrate, which leads to the presence of a layer characterized by a reduced mobility at their interfaces. We proposed a mathematical schematization of a multilayer model that allowed qualitative reproduction of the observed thickness dependences of the static and dynamic properties. In terms of such a model, the upper limit for the thickness of the reduced mobility layer was estimated as 20 nm. The conditions to extend the proposed model to different observables are finally suggested.

1. Introduction

In the past decade, the physical properties of ultrathin polymer films (thickness <200 nm) have been intensively investigated.^{1–27} Both applicative and fundamental research aim to understand the intriguing phenomena connected to the dynamics changes occurring when the thickness of a polymer film is a few tens of nanometers. As a general trend, it is observed that these changes occur when the physical dimension of the sample becomes comparable to the characteristic length scale of the investigated

material, which for a polymer is generally considered to be the gyration radius, R_g .

In this line of research, a very high number of experimental studies and theoretical models about polymeric films have investigated the variation of the glass transition temperature, T_g , that sets the processing parameters for both amorphous and semicrystalline materials (for a review, see ref 20). For several polymers, in the ultrathin regime, T_g of film of thickness h deviates from the bulk value $T_g(\infty)$ of a quantity $\Delta T_g(h)$. The amount and the sign of this variation mainly depend on two factors: the thickness of the sample h and the entity of the interfacial interaction.^{1,6,8,28} In particular, an increasing number of experimental works have focused on the influence of the substrate interaction on the properties of polymer layers at the very interface with it.

In their pioneering works on the dependence of the glass transitions on thickness, Keddie et al.^{1,28,29} noticed that, for

* Corresponding author: rolla@df.unipi.it.

[†] polyLab e Dip. Di Fisica, Università di Pisa.

[‡] NEST CNR-INFM and Scuola Normale Superiore.

[§] Dip. Ingegneria Chimica e Scienze dei Materiali, Università di Pisa.

^{||} Katholieke Universiteit Leuven.

- (1) Keddie, J. L.; Jones, R. A. L.; Cory, R. A. *Europhys. Lett.* **1994**, *27*, 59–64.
- (2) Fukao, K.; Miyamoto, Y. *Phys. Rev. E* **2000**, *61*, 1743–1754.
- (3) Dutcher, J. R.; Dalnoki-Veress, K.; Nickel, B. G.; Roth, C. B. *Macromol. Symp.* **2000**, *159*, 143–150.
- (4) Reiter, G. *Phys. Rev. Lett.* **2001**, *87*, 8718.
- (5) Dalnoki-Veress, E.; Forrester, J. A.; Murray, C.; Gigault, C.; Dutcher, J. R. *Phys. Rev. E* **2001**, *63*, 031801.
- (6) Fryer, D. S.; Peters, R. D.; Kim, E. J.; Tomaszewski, J. E.; de Pablo, J. J.; Nealey, P. F.; White, C. C.; Wu, W. L. *Macromolecules* **2001**, *34*, 5627–5634.
- (7) Fukao, K.; Uno, S.; Miyamoto, Y.; Hoshino, A.; Miyaji, H. *Phys. Rev. E* **2001**, *64*, 051807.
- (8) Tsui, O. K. C.; Russell, T. P.; Hawker, C. J. *Macromolecules* **2001**, *34*, 5535–5539.
- (9) Tate, R. S.; Fryer, D. S.; Pasqualini, S.; Montague, M. F.; de Pablo, J. J.; Nealey, P. F. *J. Chem. Phys.* **2001**, *115*, 9982–9990.
- (10) Hartmann, L.; Gorbatschow, W.; Hauwede, J.; Kremer, F. *Eur. Phys. J. E* **2002**, *8*, 145–154.
- (11) Du, B. Y.; Xie, F. C.; Wang, Y. J.; Yang, Z. Y.; Tsui, O. K. C. *Langmuir* **2002**, *18*, 8510–8517.
- (12) Serghei, A.; Kremer, F. *Phys. Rev. Lett.* **2003**, *91*, 165702.
- (13) Ellison, C. J.; Torkelson, J. M. *Nat. Mater.* **2003**, *2*, 695.
- (14) Efremov, M. Y.; Olson, E. A.; Zhang, M.; Zhang, Z.; Allen, L. H. *Phys. Rev. Lett.* **2003**, *91*, 085703.
- (15) Grohens, Y.; Hamon, L.; Spevacek, J.; Holl, Y. *Macromol. Symp.* **2003**, *203*, 155–164.
- (16) Huang, H. Y.; Zhang, F. J.; Hu, Z. J.; Du, B. Y.; He, T. B.; Lee, F. K.; Wang, Y. J.; Tsui, O. K. C. *Macromolecules* **2003**, *36*, 4084–4092.

- (17) Zhang, Y.; Zhang, J. M.; Lu, Y. L.; Duan, Y. X.; Yan, S. K.; Shen, D. Y. *Macromolecules* **2004**, *37*, 2532–2537.
- (18) Lupascu, V.; Huth, H.; Schick, C.; Wübbenhorst, M. *Thermochim. Acta* **2005**, *432*, 222–228.
- (19) Serghei, A.; Huth, H.; Schellenberger, M.; Schick, C.; Kremer, F. *Phys. Rev. E* **2005**, *71*, 061801.
- (20) Alcoutlabi, M.; McKenna, G. B. *J. Phys.: Condens. Matter* **2005**, *17*, R461–R524.
- (21) Reiter, G.; Hamieh, M.; Damman, P.; Slavovs, S.; Gabriele, S.; Vilmin, T.; Raphael, E. *Nat. Mater.* **2005**, *4*, 754–758.
- (22) Fukao, K.; Sakamoto, A. *Phys. Rev. E* **2005**, *71*, 041803.
- (23) Vignaud, G.; Bardeau, J. F.; Gibaud, A.; Grohens, Y. *Langmuir* **2005**, *21*, 8601–8604.
- (24) Tran, T. A.; Said, S.; Grohens, Y. *Macromolecules* **2005**, *38*, 3867–3871.
- (25) Tran, T. A.; Said, S.; Grohens, Y. *Composites, Part A* **2005**, *36*, 461–465.
- (26) Itagaki, H.; Nishimura, Y.; Sagisaka, E.; Grohens, Y. *Langmuir* **2006**, *22*, 742–748.
- (27) Wang, Y. J.; Tsui, O. K. C. *Langmuir* **2006**, *22*, 1959–1963.
- (28) Keddie, J. L.; Jones, R. A. L.; Cory, R. A. *Faraday Discuss.* **1994**, *219*–230.
- (29) Keddie, J. L.; Jones, R. A. L. *Isr. J. Chem.* **1995**, *35*, 21–26.

ultrathin films of polystyrene (PS), ΔT_g was almost independent from the nature of the substrate. Such a trend is not reported in samples of poly(methyl methacrylate), PMMA. In fact, films of this polymer spin-coated on gold show a negative ΔT_g , whereas positive values are reported when the films are prepared on silicon oxide, SiO_x .¹

Fryer et al. studied in detail the role of the polymer/substrate interaction.⁶ Samples of PMMA and PS were prepared on autoassembling surfaces of octadecyltrichlorosilane, OTS, on SiO_x , opportunely modified by exposing to X-rays for different elapsed times. This procedure leads to surfaces of OTS with different contents of polar groups and to samples with different polymer/surface interfacial energy values, γ_{SP} , as estimated by contact angle measurements. For low values of γ_{SP} , a negative variation from $T_g(\infty)$ was observed ($\Delta T_g < 0$). At an increase of γ_{SP} , the absolute value of ΔT_g decreases, until reaching 0 at a corresponding critical value of γ_{SP}^* . A further increase of γ_{SP} gave samples showing a positive ΔT_g . Extreme results similar to those observed in this last regime ($\Delta T_g > 0$) can be obtained via immobilization of the polymer chains by grafting them onto the substrate: Tate et al. reported, for example, that, for films of poly(4-hydroxystyrene), PHS, grafted on SiO_x , the glass transition temperature shows a positive deviation from bulk behavior of 50 K even at 100 nm.⁹

It was observed that a simple quantitative balance of the role of substrate interaction in the deviation from bulk behavior leads to nonphysical results. With a simple balance, Tsui et al.⁸ estimated that the cooperativity length scale in the case where only the interfacial energy should contribute to a deviation of T_g from the bulk behavior is on the order of tenths of angstroms, a value lower than the interatomic bond length itself. A similar balance⁸ was then used to suggest that neither acceptable density change could explain the recorded ΔT_g .

Even if not yet completely understood, the experimental observations collected until now could be used to extract guidelines for projecting polymer devices with adjustable T_g . For example, for several practical applications, it is required that the sample (or a region of it) be in a sub- T_g regime at the requested processing temperature, as such a regime is characterized by an increased resistance to acid attacks (due to lower value of the diffusivity coefficients), a strong reduction of changes in the material properties caused by temperature fluctuations, a higher barrier to gas and vapors, and so forth. A possible solution could be given by choosing appropriate preparations for the sample and the substrate that correspond to high values of ΔT_g , for example, by blocking the polymer chains by spin-coating the film on a highly interactive substrate or even, whenever possible, grafting the chains directly onto the substrate. It is thus of highly fundamental and technological interest to focus on polymer/substrate systems in which an increase of glass transition temperature is expected.

This experimental work dealt with monitoring via dielectric spectroscopy the structural relaxation of ultrathin polymer films of poly(ethylene terephthalate), PET, spin-coated on aluminum. The interfacial energy between polymer and substrate is supposed to be high due to the formation of stable chemical bonds $\text{—C=O}\cdots\text{Al}$, between aluminum surface atoms and carbonyl groups within the polymer chain, as detected both on Al/PET and AlO_x/PET interfaces.^{30–32} The analysis of relaxation dynamics supported the expectation of an increase of the glass transition

temperature induced by the presence of a polymer layer in proximity to the interface characterized by a reduced mobility.

2. Experimental Details

Poly(ethylene terephthalate) was purchased in sheets by Good-Fellow. The percentage per volume of the crystalline phase in the amorphous sheets as purchased was determined via differential scanning calorimetry, DSC, to be less than 4–5%, corresponding to the minimal value detectable with conventional DSC technique. Solutions of PET were prepared by dissolving the polymer in a mixture of chloroform and trifluoroacetic acid. Portions of the same amorphous sheet of PET used to prepare ultrathin films were cut and kept under vacuum for 3 weeks at 313 K and finally for 4 h at 353 K before being used as bulk samples (250 μm).

Ultrathin films with various thicknesses were obtained by spin-coating the solutions of polymer on cleaned glass slides, onto which an aluminum strip (50 nm thick, 0.3 mm width), used as the lower electrode, was previously thermally evaporated in a vacuum chamber (10^{-6} mbar). The temperature inside the vacuum chamber was monitored via a thermocouple sensor and always kept below 300 K in order to avoid overheating effects due to the evaporation procedure. Before metal evaporation, the glass slides were washed with a concentrated solution of sodium hydroxide in ethanol. Finally, solvent residue was removed by washing the slides with deionized water. The washing procedure was repeated at least 3 times.

Samples as prepared were kept for 72 h in a vacuum chamber (1 mbar) at 330 K (below bulk T_g ; $T_g(\infty) = 344$ K) and then for 4 h at 353 K in order to remove residual solvent and stresses induced by the spin-coating preparation.²¹ After the annealing program, a second strip of Al was deposited onto the polymer surface, following the procedure described above. The second Al layer, used as an upper electrode, is perpendicular to the lower electrode.

Ultrathin films with different thicknesses, down to 13 nm, were obtained by changing the polymer concentration. After the annealing procedure, the final thickness of the polymer layer was measured using a mechanical profilometer (Veeco), and the film quality was checked by imaging the surface using a homemade atomic force microscope. Only films with a root-mean-square (rms) roughness lower than 10% of the total polymer thickness were used for measurements.

Dielectric spectra of PET samples were collected with an Alpha high-resolution analyzer from Novocontrol. Complex capacity spectra, $C = C_0^*(\epsilon' - i\epsilon'')$, where C_0 is the empty capacity of the dielectric cell, were measured in the frequency range from 10^{-2} Hz to 10^7 Hz, under vacuum (1 mbar), and in a temperature interval that varies between 378 and 348 K depending on the film thickness. The vacuum condition kept during measurements does not influence the molecular dynamics. In fact, considering typical values of the variation of T_g with pressure for polymers, $\partial T_g/\partial P \approx 1$ K/GPa,³³ a reduction of pressure from ambient pressure to 1 mbar changes the glass transition temperature by 10^{-4} °C.

The temperature during isothermal measurements was controlled within 0.2 K by a temperature controller, model Lakeshore 311, connected to a thermoresistance in thermal contact with the sample.

3. Experimental Results

Dielectric spectra, $\epsilon = \epsilon' - i\epsilon''$, of PET were measured from 10^{-2} to 10^7 Hz and in the temperature region from above the glass transition to below it. In order to show the signal as measured, the capacity spectra, $C = C_0^*(\epsilon' - i\epsilon'')$, are presented in the text. In particular, the notation $C' = C_0^*\epsilon'$ and $C'' = C_0^*\epsilon''$, which is a positive function of the frequency, is adopted. The spectra are characterized by two distinct relaxation phenomena, the structural α -peak related to the dynamic glass transition, and a secondary β -peak appearing at higher frequencies in the glassy

(30) Cueff, R.; Baud, G.; Benmalek, M.; Besse, J. P.; Butruille, J. R.; Jacquet, M. *Surf. Coat. Technol.* **1996**, *80*, 96–99.

(31) Le, Q. T.; Pireaux, J. J.; Caudano, R.; Leclerc, P.; Lazzaroni, R. *J. Adhes. Sci. Technol.* **1998**, *12*, 999–1023.

(32) Sandrin, L.; Sacher, E. *Appl. Surf. Sci.* **1998**, *135*, 339–349.

(33) Donth, E. *The Glass Transition, Relaxation Dynamics in Liquids and Disordered Materials*; Springer-Verlag: New York, 2001.

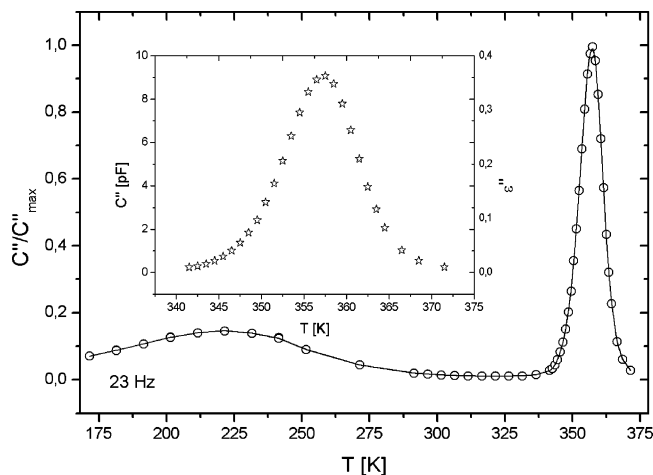


Figure 1. Isochronal representation at 23 Hz of the imaginary part of the complex capacity C'' for a 250- μm -thick film. The two relaxation contributions can be observed: the structural and the secondary processes appearing at high and low temperature, respectively. In the inset is a detail on the structural relaxation. The line is a guide for eyes.

state. In an isochronal representation (Figure 1), the α -peak appears at higher temperature than the β -peak. In this article, we will consider only dynamics above T_g , i.e., the structural peak. Besides these relaxation contributions, the spectra of ultrathin polymer films show two more features: at low frequencies the conductivity contribution, mainly due to the residuals of ionic impurities trapped during the preparation of the sample, and at high frequency an instrumental temperature-independent peak, due to the resistance of the metallic electrodes. The conductivity contribution is more significant in the thinnest film where it partially covers the structural peak at low temperatures, interfering with the analysis of the relaxation process. In order to extend the frequency range of analysis toward lower frequencies, we considered the loss spectra as calculated by the following relation³⁴

$$C''(\omega) \propto -\frac{\pi}{2} \frac{dC'(\omega)}{d \ln \omega} \quad (1)$$

which is valid since C' and C'' are Kramers–Kronig related functions. Since the conductivity contribution affects only the imaginary part of the spectra, the loss spectra calculated through eq 1 are not affected by the conductivity contribution of free ions (Figure 2). The above equation is derived under the approximation of flat distribution of relaxation times. For a more detailed discussion on this approximation, the reader can refer to refs 34 and 35. The validity of this approximation in our case was verified with dielectric spectra of the film at 85 nm.

Despite the attempt to correct for the above contribution, the analysis of relaxation dynamics in the thin film was limited to the frequency interval from 10 to 10^5 Hz. The structural relaxation peak was reproduced by means of the Havriliak Negami, HN, equation

$$C(\omega) - C_\infty = \frac{\Delta C}{[1 + (i\omega\tau)^{1-\alpha}]^\beta} \quad (2)$$

where $\Delta C = C_0\Delta\epsilon$ is related to the dielectric relaxation strength, $\Delta\epsilon$, of the process; τ is the characteristic time; α and β are the

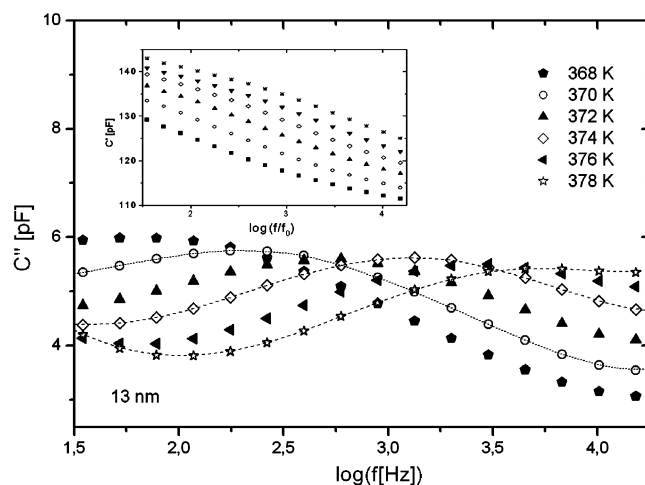


Figure 2. Dielectric spectra of a 13-nm-thick film of PET, at the different temperatures listed in the figure. The spectra were corrected for the contribution of electric conductivity (see text for details).

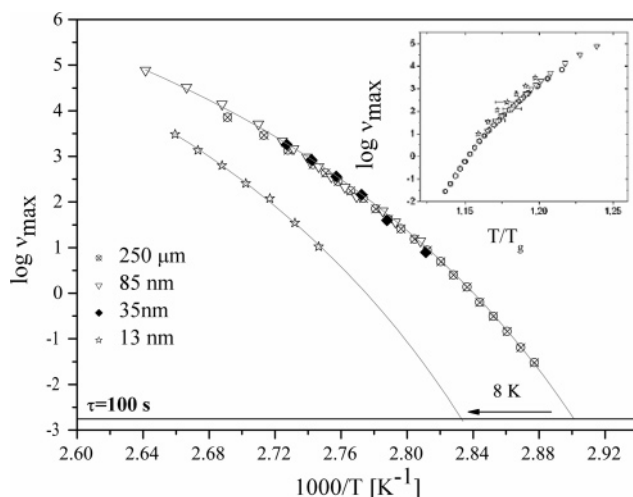


Figure 3. Logarithmic of the maximum frequency as a function of $1000/T$, as calculated from the fit of the loss spectra of the different films. In the inset, the same curves were superimposed by rescaling the temperature by the Vogel temperature T_0 (values in Table 1).

parameters related to the broadness and the asymmetry of the peak; and $C_\infty = C_0\epsilon_\infty$. As a model independent parameter characterizing the time scale of the relaxation process, the frequency of the maximum of the loss peak, ν_{\max} , was chosen, as calculated through

$$\nu_{\max}(T) = \frac{1}{2\pi\tau} \left\{ \sin \left[\frac{(1-\alpha)\pi}{2+2\beta} \right] \right\}^{\frac{1}{1-\alpha}} \left\{ \sin \left[\frac{(1-\alpha)\beta\pi}{2+2\beta} \right] \right\}^{-\frac{1}{1-\alpha}} \quad (3)$$

with the parameters determined by eq 2 (Figure 3). The temperature dependence of ν_{\max} was fitted with the Vogel Fulcher Tamman, VFT, equation

$$\nu_{\max}(T) = \nu_0 \exp \left(-\frac{DT_0}{T - T_0} \right) \quad (4)$$

where T_0 is the Vogel temperature, D is a parameter related to the curvature of the $\nu_{\max}(T)$ curve, and ν_0 is the relaxation frequency in the limit of infinite temperature. In Table 1, the values of the parameters of the VFT equation for each film are reported, together with the value of T_g , defined as the temperature

(34) Bottcher, C. *Theory of Dielectric Polarization*; Elsevier Scientific Publishing Company: Amsterdam, 1973.

(35) Wübbenhorst, M.; van Turnhout, J. J. *Non-Cryst. Solids* **2002**, 305, 40–49.

Table 1. ^a

	$\log \nu_0$	D	T_0	m	T_g
250 μm	13.6 ± 0.3	4.81 ± 0.02	305.6 ± 0.5	146 ± 10	344.0 ± 0.5
85 nm	13.6 ± 0.4	4.6 ± 0.1	305.7 ± 0.7	142 ± 10	344 ± 1
13 nm	13.6 ± 0.5	4.8 ± 0.1	314 ± 1	156 ± 10	352 ± 2

^a First three columns: parameters of the VFT Fit of the $\nu_\alpha(T)$ curves. Last two columns: the values of the fragility, m , and the glass transition temperature, T_g , calculated from the formers.

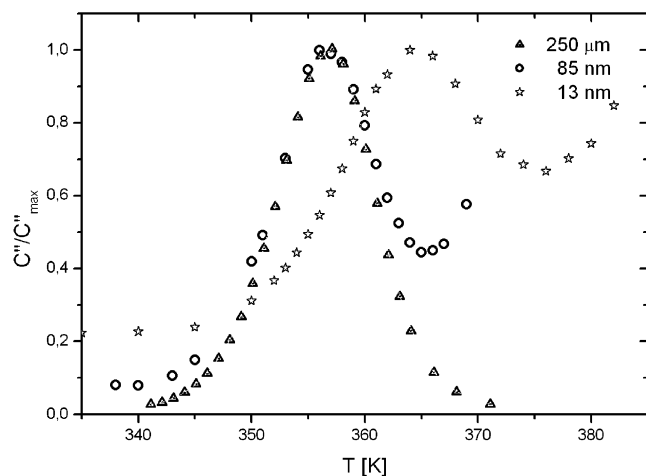


Figure 4. Isochronal representation at 23 Hz of the imaginary part of the complex capacity C'' (symbols) for films of different thicknesses. The line is a guide for the eyes. The data were normalized to the maximum value of the α -peak, C''_{\max} . For clarity, only data for films at three values of thickness are represented.

at which $\nu_{\max} = 1/(2\pi 100)$ Hz, and the value of the fragility parameter m .³³

Figure 4 shows an isochronal representation at 23 Hz of the imaginary part of the complex capacity C'' , normalized to the maximum value of the α -peak, C''_{\max} , for films of different thicknesses. The temperature at which the structural relaxation, in such a representation, shows a maximum will be indicated with T_α ($T_g \equiv T_\alpha$ when $\nu_{\max} = 1/(2\pi 100)$ Hz). The α -peak in 85-nm-thick films completely overlaps that measured for 250 μm films, except for an increase at higher temperatures. However, this increase is mainly due to the conductivity contribution that in thin films is greater relative to the α -peak than in a thick sample. The peak corresponding to the structural relaxation for 13-nm-thick films is shifted by 8 K toward higher temperatures than in the bulk. In an isothermal representation of C''/C''_{\max} (Figure 4), this corresponds to a shift of the α relaxation peak toward lower frequencies, i.e., a slowing down of the molecular dynamics connected to the structural relaxation.

Estimations of interfacial energy between PET and aluminum were performed by means of contact angle measurements. A CAM 200 optical contact angle meter goniometer by KSV was used to measure diodomethane, water, and glycerol (purchased from Aldrich) static contact angles of 5 mL droplets on the surface of an aluminum substrate. The droplets were formed at a rate of 0.2 mL/s, and two different images were recorded for each drop. An average value was obtained from five measurements for each sample.

Contact angles, θ , of the three liquids were used to calculate the dispersive, γ_s^{LW} , and polar, γ_s^{p} , contributions of the surface

Table 2. Contact Angle Values of the Test Liquids with Al Substrates

	diodomethane	water	glycerol
Al	63.6 ± 0.1	79.0 ± 0.7	74 ± 2

energy of the substrate according to the Young–Dupré equation³⁶

$$(1 + \cos\theta)\gamma_s = 2[(\gamma_s^{\text{LW}} \gamma_l^{\text{LW}})^{1/2} + (\gamma_s^+ \gamma_l^-)^{1/2} + (\gamma_s^- \gamma_l^+)^{1/2}] \quad (5)$$

where the subscript l refers to the liquid, and the polar contribution of the surface energy is expressed in terms of electron acceptor and electron donor terms $\gamma^{\text{p}} = (\gamma^+ \gamma^-)^{1/2}$.³⁶ The values of the surface energies for the liquids and PET were previously determined.³⁷ The Good–Girifalco–Fowkes combining rule was applied to estimate the interfacial energy, γ_{sp} , between PET and Al³⁸

$$\gamma_{\text{sp}} = (\sqrt{\gamma_s^{\text{LW}}} - \sqrt{\gamma_p^{\text{LW}}})^2 + 2[(\gamma_s^+ \gamma_p^-)^{1/2} + (\gamma_p^+ \gamma_s^-)^{1/2} - (\gamma_s^+ \gamma_p^-)^{1/2} - (\gamma_p^+ \gamma_s^-)^{1/2}] \quad (6)$$

where p and s refer to the polymer and substrate, respectively. The results for contact angle measurements are shown in Table 2. The dispersive contribution of the PET/Al interfacial energy, i.e., the first term in eq 6, is 2.1 ± 0.1 mJ/m², and the polar one is 0.9 ± 0.2 mJ/m², for a total energy of 3 ± 0.3 mJ/m². In comparison to the values calculated in ref 6, for different couples of substrates and polymer, the value here found is higher³⁹ and is in the region related to an increase of T_g corresponding to a slowing down of the relaxation dynamics.

4. Discussion

4.1. Influence of Annealing on Cold Crystallization. In order to eliminate any residual solvent after spin-coating, the ultrathin films were subjected to an adequate annealing procedure. Traces of residual solvent could act as a plasticizer and reduce the value of T_g of the system, masking or influencing the eventual changes induced by interfacial effects. Such a step does not require any particular precaution in glassy polymers, as long as the annealing temperature T_A is taken below the high-temperature region in which the polymer degrades. This process has to be performed in ultrahigh vacuum or controlled atmosphere in order to prevent any contamination.

In semicrystalline polymers, the annealing procedure requires a more accurate projecting phase: in the case that the crystalline volume fraction is required to be constant, the annealing conditions should be chosen in order to avoid any crystallization phenomena. As crystallization can occur at every temperature between T_g and T_m , when choosing an annealing temperature, the maximum heating time, t_A , before crystallization starts should be known.

(37) Lee, L. H. *Langmuir* **1996**, *12*, 1681–1687.

(38) Good, R. J.; Girifalco, L. A. *J. Chem. Phys.* **1960**, *64*, 561–565.

(39) The value found here is expected to be lower than the real interface energy, as the model used is not taking in account the full contribution from the chemical bond reported in refs 22–24.

(36) Vanoss, C. J.; Chaudhury, M. K.; Good, R. J. *Chem. Rev.* **1988**, *88*, 927–941.

In a bulk sample of PET annealed at 359 K, the percentage per volume of amorphous phase begins to decrease after only 15 h.⁴⁰ Ultrathin films (down to 20 nm) of PET prepared from a solution of polymer dissolved in chloroform and trifluoroacetic acid remained amorphous after 4 h annealing at 357 K.¹⁷

Dielectric spectra of films prepared according to the preparation procedure reported in ref 17 showed the same trend: In Figure 4, at 85 nm the structural relaxation of the thin film perfectly overlapped that of a bulk film not obtained by spin-coating. The annealing procedure was thus sufficient to remove the solvent and did not induce any crystallization phenomena (crystalline samples would show a slower α -relaxation). Thinner films are expected to be amorphous, as it was widely proven that a reduction of the thickness leads to an increase of the sample resistance against cold crystallization.^{41–43}

4.2. Influence of Confinement on the Relaxation Dynamics. Interfacial effects play a fundamental role in the dynamic properties of ultrathin polymer films and in general of all confined systems. The dielectric relaxation of ultrathin films of PET spin-coated on aluminum down to 35 nm is characterized by the same relaxation properties as the bulk. However, for 13-nm-thick films, a reduction of mobility of the chain is observed, quantitatively as an increase of T_g of 8 K (Table 1) and an increase of 8 K of T_α (23 Hz), i.e., the temperature at which the maximum of the structural peak is observed in an isochronal representation of the spectra at 23 Hz (Figure 4). As can be deduced by the equal variation with thickness of the values of T_α and T_g , the reduction of mobility in thinner samples of PET occurred independently from the dynamic range where the structural relaxation was observed. This result is confirmed also by the rescaled Arrhenius plot (inset of Figure 3), where the $\nu_{\max}(T)$ curves for films of different thicknesses can be superposed simply by a horizontal shift, and by the calculated values of fragility that are independent of thickness (Table 1).

Fourier transform spectroscopy measurements of PET ultrathin films supported on a gold substrate revealed a variation from bulk behavior even for thicker samples (around 60 nm)¹⁷ and a decrease of the glass transition temperature of more than 20 K at 25 nm. The apparent discrepancy is probably due to the different way the two techniques assign T_g : the analysis of dielectric relaxation spectra focuses on the thermal evolution of the structural relaxation, while a value of T_g can be extracted by FTIR spectra in terms of changes of chain conformation bands. It is already reported that even techniques giving similar results for bulk samples could show divergent trends in the nanoscale.²⁰

The observed decrease of molecular mobility can be explained in terms of a multilayer model. Due to a relatively high interfacial energy between PET and Al (3 mJ/m²), the layer of polymer at the very interface with the lower electrode, often referred as a dead layer,⁴⁴ is characterized by the absence of molecular mobility on the time and length scale of the dynamic glass transition. Modeling a change of the static and dynamical properties of the film along the thickness,^{23,45,46} we can assume that the polymer layers in proximity to the dead layer will show reduced mobility. We refer to it as the reduced mobility layer, RML, indicating the region next to an interface in which the long-range interaction

of the substrate influences the sample properties. The extension of the RML depends on the entity of the substrate interaction and the flexibility of the polymer chains. Polymers with less flexible chains are expected to have a thicker RML. In these terms, the reduced mobility layer could be compared to the rigid amorphous fraction of a semicrystalline material, i.e., the region at the interface between the immobilized crystalline chains and the mobile amorphous phase, which shows intermediate properties between the two.^{47–49}

With the dimension of the RML considered constant, and the interface interaction being constant, a reduction of the thickness corresponds to an increase of the percentage of the total film occupied by RML and thus to a bigger effect of confinement. For bulk samples, for which the extension of the RML over the whole thickness is negligible, no effect is observed.

The presence of a layer with a different mobility can explain not only the slowdown of the mobility but also the observed broadening of the α -relaxation loss peak (Figure 4). In fact, the RML introduces a heterogeneity element into the relaxation dynamics, and the polymer chains inside or close to it are expected to move more slowly than the chains far from the interface. The presence of these slower chains produces a broadening of the distribution of relaxation time toward lower values, which is reflected in a broadening and a shift of the peak toward smaller frequencies. According to this hypothesis, the broadening of the peak should be asymmetric, but the occurrence of the conductivity contribution does not allow a more detailed investigation of this aspect. Finally, we also observed a decreasing of the dielectric strength with thickness of about 70% in accordance with previous works on different systems.^{10,44} Such variation can be explained in terms of the presence of an RML where the chains suffer for stronger geometrical constraints, thus contributing to a lesser extent of the dissipation of energy.

Quantitatively, a multilayer schematization for polymeric films, one RML at each interface and a bulk layer of thickness ($h - d$) in between, provides that the measured dielectric signal can be written as

$$\epsilon(\omega, T) = h^* \frac{\epsilon_b(\omega, T) \cdot \epsilon_d(\omega, T)}{d^* \epsilon_b(\omega, T) + (h - d) \epsilon_d(\omega, T)} \quad (7)$$

where $\epsilon_b(\omega, T)$ is the permittivity of the bulk and $\epsilon_d(\omega, T)$ and d the permittivity and the total thickness of the RML. The above expression is calculated with the assumption that the RML and bulk layers do not interpenetrate each other. We remark that in such a schematization d is the total thickness of the RML zone, irrespective of its distribution in the sample: in case an RML exists only at the interface with the lower electrode, d is its thickness.

Dielectric spectra of films of any thickness value can be calculated by eq 7 once the contributions of the bulk and RML and their thicknesses are known. As a first approximation, we used the shape parameters and the temperature dependence of the relaxation frequency of the structural process of the 13 nm film as representative of those of the RML. This approximation limits the validity of the simulation when h/d is close to unity. Through the dielectric spectra, simulated at different values of thickness and temperature, we calculated the thickness dependence of the dielectric strength, $\Delta\epsilon$, of the structural process, and that of the temperature at which the maximum of the structural

(40) Fukao, K.; Miyamoto, Y. *J. Non-Cryst. Solids* **1997**, 212, 208–214.

(41) Despotopoulou, M. M.; Frank, C. W.; Miller, R. D.; Rabolt, J. F. *Macromolecules* **1996**, 29, 5797–5804.

(42) Zhang, Y.; Lu, Y. L.; Duan, Y. X.; Zhang, J. M.; Yan, S. K.; Shen, D. Y. *J. Polym. Sci. Part B: Polym. Phys.* **2004**, 42, 4440–4447.

(43) Capitan, M. J.; Rueda, D. R.; Ezquerro, T. A. *Macromolecules* **2004**, 37, 5653–5659.

(44) Fukao, K.; Miyamoto, Y. *Phys. Rev. E* **2001**, 64, 011803.

(45) Kim, J. H.; Jang, J.; Zin, W. C. *Langmuir* **2000**, 16, 4064–4067.

(46) Kim, J. H.; Jang, J.; Zin, W. C. *Langmuir* **2001**, 17, 2703–2710.

(47) Boyer, R. F. *Macromolecules* **1973**, 6, 288–299.

(48) Schick, C.; Wurm, A.; Mohammed, A. *Thermochim. Acta* **2003**, 396, 119–132.

(49) Alsleben, M.; Schick, C. *Thermochim. Acta* **1994**, 238, 203–227.

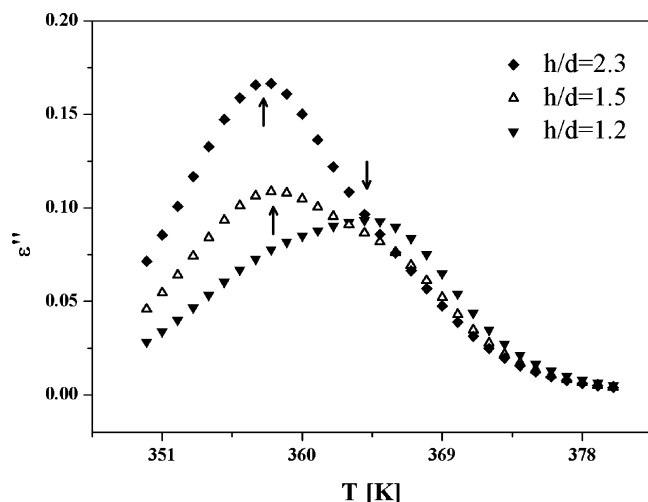


Figure 5. Isochronal (100 Hz) spectra of PET film for various relative thicknesses (reported in the figure) as calculated from eq 6. The arrows indicate the positions of the peaks.

loss peak reaches a fixed value of frequency. The latter was calculated by simulated isochronal spectra at 100 Hz (Figure 5). It is important to note that spectra calculated by eq 7 can show two peaks, one for each contribution, for certain values of thickness. However, in the simulated isothermal spectra, the two peaks appear only at low-temperature frequency values, close to T_g , and for thicknesses of the film close to that of the reduced mobility layer. At high frequency, as represented in isochronal spectra at 100 Hz, the two contributions are not separated but appear as a single broad peak. In the experimental spectra, the presence of the conductivity contribution avoids the observation of the second peak.

The simulation of the thickness dependence of the temperature at which the maximum loss peak reaches the frequency of 100 Hz (Figure 6a) evidences that about 90% of the total variation of the dynamics occurs for a small variation of thicknesses, namely, from $1.5d$ to d . The prediction of such a sharp transition is in qualitative agreement with the fast variation of dynamics usually observed in other systems.^{2,50} The discrepancies with other experimental results, evidencing variation of dynamics over a broader interval of thickness,² can be due to the rough schematization leading to eq 7 and to the presence of other phenomena inducing the dynamic variation. Despite its approximate nature, eq 7 can be used to estimate the dimension of the RML. Since our data at 35 nm do not evidence variation of dynamics from the bulk (Figure 3), we can conclude that the RML for PET films capped between Al electrodes should be ≤ 20 nm.

The thickness dependence of $\Delta\epsilon$ shows a different behavior (Figure 6b). The variation with respect to the bulk properties in this quantity can be observed at larger values of thickness than for dielectric dynamics properties, and variation of 10% can be observed for thicknesses on the order of $10 \times d$. The trend modeled by eq 7 qualitatively reproduces the experimental observations for ultrathin films of PET (Figure 7).

Finally, even if eq 7 is obtained for the dielectric response, it can be generalized to interpret the data by other experimental techniques working in the linear response regime. In particular, indicating with $X(\omega, T)$ the generalized displacement associated to the generalized force $\Gamma(\omega, T)$, we can define a generalized modulus $M(\omega, T) = X(\omega, T)/\Gamma(\omega, T)$. Equation 7 can be thus

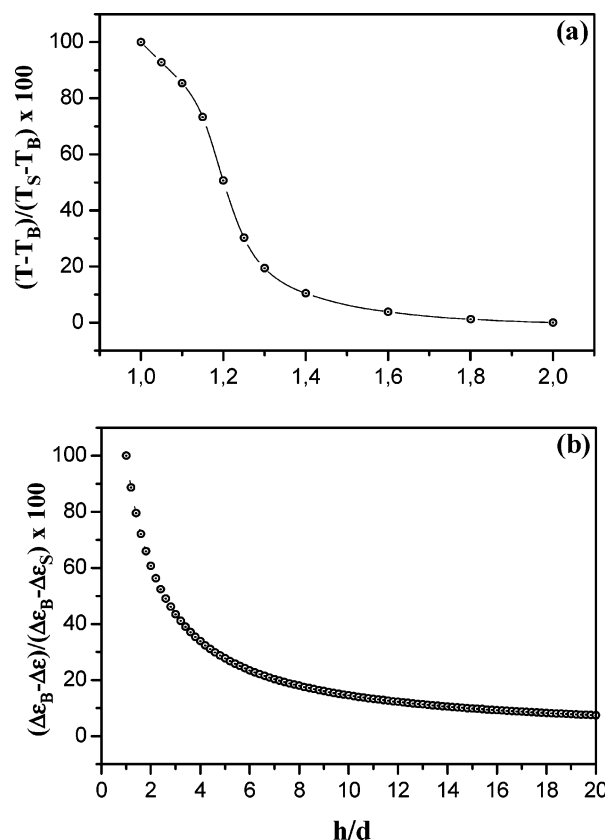


Figure 6. Simulation of the thickness dependence of dielectric properties. As a function of the ratio of the total thickness over that of the reduced mobility layer, we report (a) the relative variation of the temperature, T , at which the maximum loss reaches 100 Hz and (b) the relative variation of the dielectric strength of the structural process, $\Delta\epsilon$. The subscript B refers to the bulk; the subscript S refers to the reduced mobility layer.

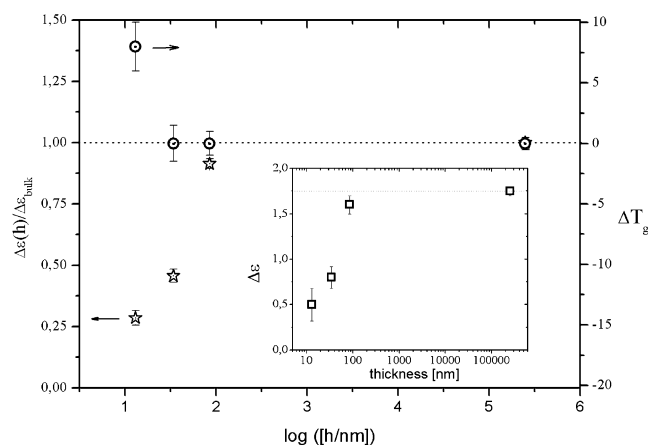


Figure 7. Dependence on thickness of the deviation from bulk behavior for the glass transition temperature, T_g , and the dielectric strength of the structural process, $\Delta\epsilon$. In the inset is the drop of the absolute value of $\Delta\epsilon$ as a function of the thickness.

generalized for the modulus as

$$M(\omega, T) = h^* \frac{M_b(\omega, T) \cdot M_d(\omega, T)}{d \cdot M_b(\omega, T) + (h - d) M_d(\omega, T)} \quad (8)$$

and used to monitor the changes induced by a layer with a different mobility in proximity of an interface in the spectra of ultrathin polymer films. Equation 8 is valid in the case where the generalized displacement is an extensive property of the system

(50) Wübbenhorst, M.; Murray, C. A.; Dutcher, J. R. *Eur. Phys. J. E* **2003**, 12, S109–S112.

and Γ is constant within the system and applied parallel to the confinement direction, as, for example, in the case of mechanical measurements.

5. Conclusions

We presented dielectric relaxation measurements above the glass transition temperature of amorphous poly(ethylene terephthalate) films of thicknesses between 250 μm and 13 nm. The investigated films were capped between aluminum electrodes. The spectra clearly show that the structural dynamics is slowed down when the thickness is reduced to 13 nm. The reduction of mobility is about 8 K over the dynamic range from 10^4 to 10^1 Hz, and this result can probably be considered valid over a wider dynamic range. This result is explained in terms of multilayers models, assuming the presence of a reduced mobility layer at the very interface between the metal and the polymer. This explanation is supported by the broadening of the structural peak observed for the thinnest film, the decrease in dielectric strength, and from contact angle measurements indicating a relatively high interfacial interaction between aluminum and polymer. Finally, the observed results evidence that the confinement is more effective in reducing the dielectric strength than in varying the dynamics of the structural process of the thin film. In fact,

the variation of dielectric strength can be observed for larger values of thicknesses than that of the relaxation dynamics. Besides the qualitative interpretation of the results in terms of a multilayer model, we proposed a more quantitative one. Such an analysis supported the results about the thickness dependence of the dielectric strength and of the dynamics of the structural process. Moreover, it allowed an estimation of the upper limit of about 20 nm for the thickness of the reduced mobility layer. The proposed schematization can be extended to other observables measured in the linear response regime under definite conditions.

Acknowledgment. Financial support by MIUR–FIRB 2003 D.D.2186 is kindly acknowledged. The authors acknowledge Dr. S. Capaccioli, Ms. Elisa Martinelli, and Prof. Emo Chiellini for contact angle measurements. Dr. S. Capaccioli is also acknowledged for helpful discussion on polymer dynamics. Ms. M. Lucci is acknowledged for the calculus of interfacial energy values.

Supporting Information Available: Additional experimental data. This material is available free of charge via the Internet at <http://pubs.acs.org>.

LA062229J